

Optical-model analysis of $^{14}\text{C} + ^{14}\text{C}$ elastic scattering using deep potential

Shashi Verma^a and Raghuvir Singh

Department of Physics and Astrophysics, Delhi University, Delhi-110007, India

Received: 19 April 2004 / Revised version: 21 July 2004 /

Published online: 6 December 2004 – © Società Italiana di Fisica / Springer-Verlag 2004

Communicated by A. Molinari

Abstract. An optical-model analysis of the $^{14}\text{C} + ^{14}\text{C}$ elastic-scattering data has been carried out in terms of optical potential with a deep real part. The angular distributions at a number of incident energies and the excitation functions at $\theta_{\text{cm}} = 70^\circ, 80^\circ$ and 90° in the $6 \leq E_{\text{cm}} \leq 35$ MeV energy range have been described quite successfully.

PACS. 24.10.Ht Optical and diffraction models – 25.70.Bc Elastic and quasielastic scattering – 25.70.Ef Resonances

1 Introduction

Experimental investigations involving heavy-ion elastic scattering led to the observation of resonance-like structures in the excitation functions of a number of systems [1,2]. Among the identical heavy-ion systems, $^{16}\text{O} + ^{16}\text{O}$ [3] and $^{14}\text{C} + ^{14}\text{C}$ [4,5] exhibit perhaps the most pronounced and regular structures in their $\theta_{\text{cm}} = 90^\circ$ elastic scattering excitation functions. An optical-model analysis of $^{12}\text{C} + ^{12}\text{C}$ elastic scattering data between $E_{\text{cm}} = 35$ and 63 MeV indicated that the nuclear potential for this system in the region of large overlap was much deeper than expected [6]. Earlier optical-model analysis of the $^{16}\text{O} + ^{16}\text{O}$ elastic data showed that the surface transparent [3,7] and J -dependent [8] potentials could explain these data reasonably well. The same was true of the $^{14}\text{C} + ^{14}\text{C}$ elastic data [4]. These phenomenological potentials were basically shallow.

Some time ago Kondo *et al.* [9] re-examined the $^{16}\text{O} + ^{16}\text{O}$ elastic and fusion data in the energy range $15 < E_{\text{cm}} < 40$ MeV within the optical-model framework in view of the results of the semiclassical analysis [10] of non-local nucleus-nucleus interaction obtained following the resonating group method. It was suggested that the equivalent local interaction for $^{16}\text{O} + ^{16}\text{O}$ like heavy-ion systems should assume the form of a deep potential which could support wave functions with a proper number of radial nodes. Such a potential is expected to manifest itself in weakly absorbing heavy-ion systems for which nuclear scattering is sensitive to the short-range part of the ion-ion interaction, and these are precisely the systems

that exhibit resonant structures which can be described in terms of surface transparent absorptive potentials [11]. Like at higher energies [12–14], such deep potentials have been successful in describing the elastic data in the lower energy range where the shallow potentials are also available. In fact, at $E_{\text{lab}} = 350$ MeV Kondo *et al.* [12] found a unique deep potential for the $^{16}\text{O} + ^{16}\text{O}$ system. Very recently Ohkubo [15] has demonstrated that rainbow scattering and molecular structure of the $^{16}\text{O} + ^{16}\text{O}$ system can be described in a unified way with a global deep potential. As a matter of fact, Branden and Satchler [14] have pointed out that through careful studies of light heavy-ion systems physically realistic potentials have been unambiguously determined to be indeed deep. The imaginary parts of these optical potentials are shallow. Analysis of elastic scattering of $^{16}\text{O} + ^{16}\text{O}$ at energies between 5 and 8 MeV/nucleon showed that the data could be described by the real potentials which are similar to the ones required at higher energies for this and other light systems [16]. With deep real parts (300–400 MeV at the center) a rather weak absorption is required [16]. The latter is, of course, in accord with the low number of outgoing channels available to carry away the incident flux for systems like $^{16}\text{O} + ^{16}\text{O}$ [16]. The success of deep optical potentials for describing low-energy elastic and fusion data for $^{16}\text{O} + ^{16}\text{O}$ [9] and $^{16}\text{O} + ^{12}\text{C}$ [17] systems suggests that deep potentials should be valid for a wider range of heavy-ion systems.

There exists striking resemblance between the $^{16}\text{O} + ^{16}\text{O}$ and $^{14}\text{C} + ^{14}\text{C}$ elastic data [4] on excitation functions and angular distributions. In fact, the similarity in the behavior of the data reflects similar dynamical conditions prevailing during the $^{16}\text{O} + ^{16}\text{O}$ and $^{14}\text{C} + ^{14}\text{C}$

^a e-mail: vermasvin@rediffmail.com

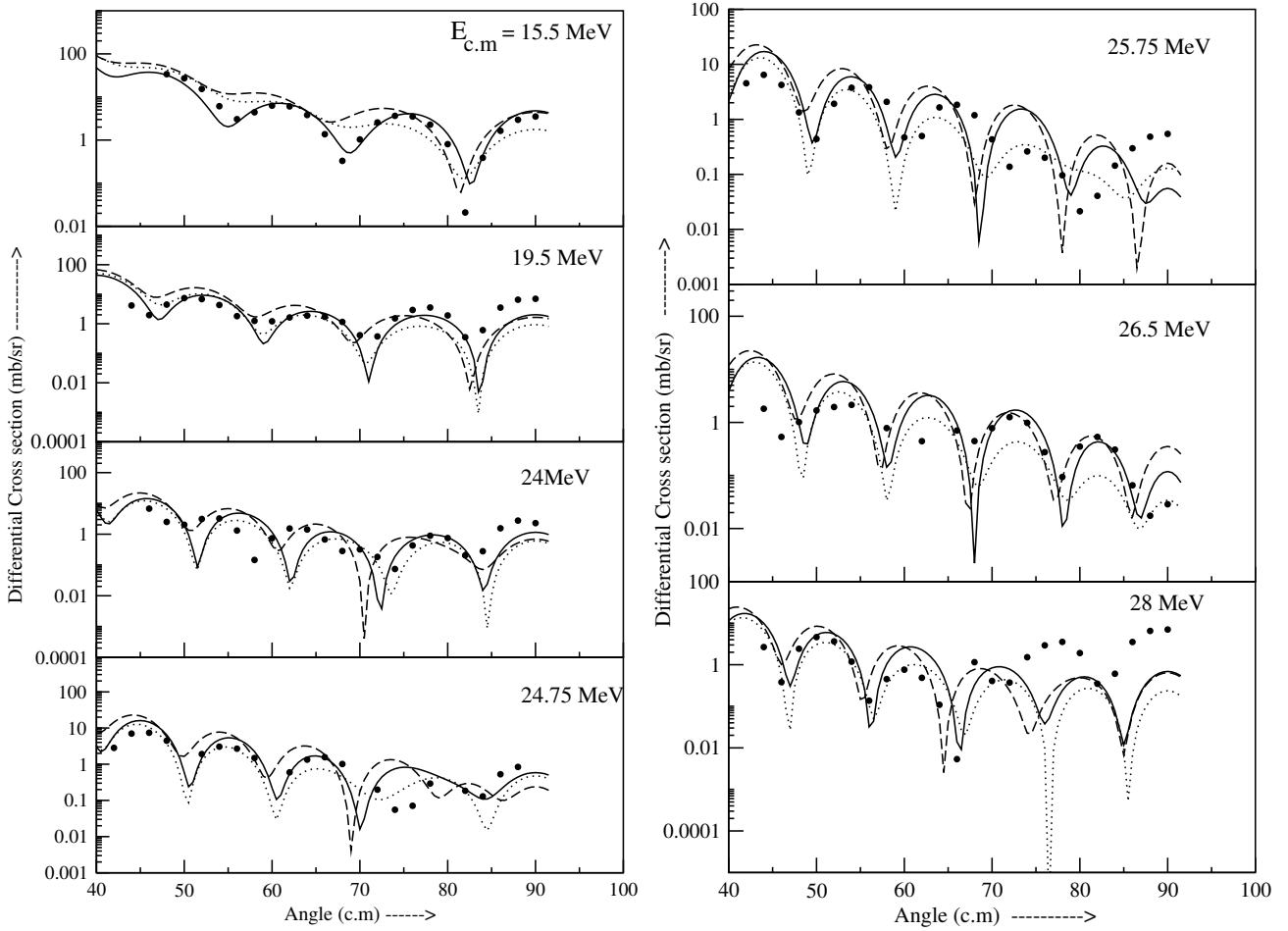


Fig. 1. Experimental and theoretical $^{14}\text{C} + ^{14}\text{C}$ elastic-scattering angular distributions at energies indicated in the panels. The continuous curves result from Set I, the dotted curves from Set II and the dashed curves from Set III of the parameters given in table 1.

Table 1. The $^{14}\text{C} + ^{14}\text{C}$ optical-model parameters obtained using deep (Set I), shallow surface transparent (Set II) and shallow J -dependent (Set III) potentials.

Set	V_o (MeV)	r_r (fm)	a_r (fm)	V_j (MeV)	W (MeV)	r_i (fm)	a_i (fm)	\bar{R} (fm)	\bar{Q} (fm)	ΔJ
I	260	0.9606	1.28	0.09	$4 + 0.3E_{\text{cm}}$	1.39	0.40	7.7	6.73	1
II	17	1.35	0.49	–	$1.5 + 0.5E_{\text{cm}}$	1.27	0.49	–	–	–
III	17	1.35	0.49	–	$7 + 0.4E_{\text{cm}}$	1.35	0.49	7.7	6.73	1

collisions. It is, therefore, expected that like $^{16}\text{O} + ^{16}\text{O}$, the elastic scattering data on $^{14}\text{C} + ^{14}\text{C}$ can also be explained in terms of a deep real optical potential. Here we have attempted the same by re-examining the $^{14}\text{C} + ^{14}\text{C}$ elastic data through an optical-model analysis.

2 Analysis

Konnerth *et al.* [4] had measured the $^{14}\text{C} + ^{14}\text{C}$ elastic scattering cross-sections at 70° , 80° and 90° (c.m.) in the energy range between 6 and 35 MeV (c.m.). The 90° excitation function exhibits strongly pronounced and regular gross structure with peaks at $E_{\text{cm}} = 15.5, 19.5, 24.0$ and

28.0 MeV. The peak-to-valley ratios exceed an order of magnitude and widths are of the order of 2–3 MeV. The excitation functions at 70° and, in particular at 80° are less regular and somewhat more fragmented than that at 90° [4]. The elastic-scattering angular distributions were measured at $E_{\text{cm}} = 15.5, 19.5, 24.0$ and 28.0 MeV (the maxima in the $\theta_{\text{cm}} = 90^\circ$ excitation function) and $E_{\text{cm}} = 24.75$ and 26.5 MeV (at the two minima) and $E_{\text{cm}} = 25.75$ MeV (an intermediate energy) [4]. These are the data that have been subjected to the optical-model analysis.

For the present analysis the optical-model code HIGENOA [18] was employed. Different kinds of

optical-potential forms were incorporated by appropriately modifying this code. The accuracy of the results obtained with the code was verified by reproducing the predictions for excitation functions and angular distributions for $^{16}\text{O} + ^{16}\text{O}$ elastic scattering using different forms of phenomenological optical potentials reported in ref. [9].

In order to search for the deep optical potential for $^{14}\text{C} + ^{14}\text{C}$ scattering, we have adopted the same approach as followed by Kondo *et al.* [9] for $^{16}\text{O} + ^{16}\text{O}$. The optical potential was of the following form:

$$U(r) = V_c(R_c, r) + [V_o + V_j J(J+1)][g(R_r, a_r, r)]^2 + iW(E_{\text{cm}}, J)g(R_i, a_i, r) \quad (1)$$

with

$$W(E_{\text{cm}}, J) = (W_o + W_E E_{\text{cm}})\{1 + \exp[(J - J_c)/\Delta J]\}^{-1}, \quad (2)$$

$$g(R, a, r) = [1 + \exp[(r - R)/a]]^{-1}. \quad (3)$$

Here, $V_c(R_c, r)$ is the Coulomb potential for a uniform charge distribution of radius R_c , V_o and V_j describe a J -dependent real potential depth where J is the total angular momentum, W_o and W_E describe an energy-dependent absorptive potential, J_c is the cut-off angular momentum applied to the absorptive term and ΔJ is the diffuseness parameter associated with cut-off [8].

At each energy, J_c is parametrized as

$$J_c = \bar{R}[(2\mu/\hbar^2)(E_{\text{cm}} - \bar{Q})]^{1/2} \quad (4)$$

with \bar{R} as the average radius and \bar{Q} as the threshold energy corresponding to the predominant non-elastic reactions and μ as the reduced mass of the system. The real part of the potential $U(r)$ has a squared Woods-Saxon form factor with radius R_r and diffuseness a_r . The imaginary part has a conventional Woods-Saxon form with radius R_i and diffuseness a_i .

Thus the real part has a form closer to the double folding model. The double folding model [19] with a realistic nucleon-nucleon interaction, predicts deep potentials but does not take into account the Pauli principle fully. The double-folding model calculations using the DDM3Y effective interaction produce angular distributions similar to the results of the potential obtained for the $^{16}\text{O} + ^{16}\text{O}$ system [12]. The fittings to the $^{14}\text{C} + ^{14}\text{C}$ scattering data have been obtained by systematically varying as few parameters as possible of the optical potential derived for $^{16}\text{O} + ^{16}\text{O}$ scattering. This way fine tuning of parameters resulted in deep potential parameters for $^{14}\text{C} + ^{14}\text{C}$ (see Set I of table 1).

3 Results and discussion

The potential parameters, obtained following the above-mentioned procedure, give quite reasonable fits to the $^{14}\text{C} + ^{14}\text{C}$ scattering data. Experimental and theoretical angular distributions, at the energies corresponding to the maxima (15.5, 19.5, 24.0, 28.0 MeV) in the 90° excitation

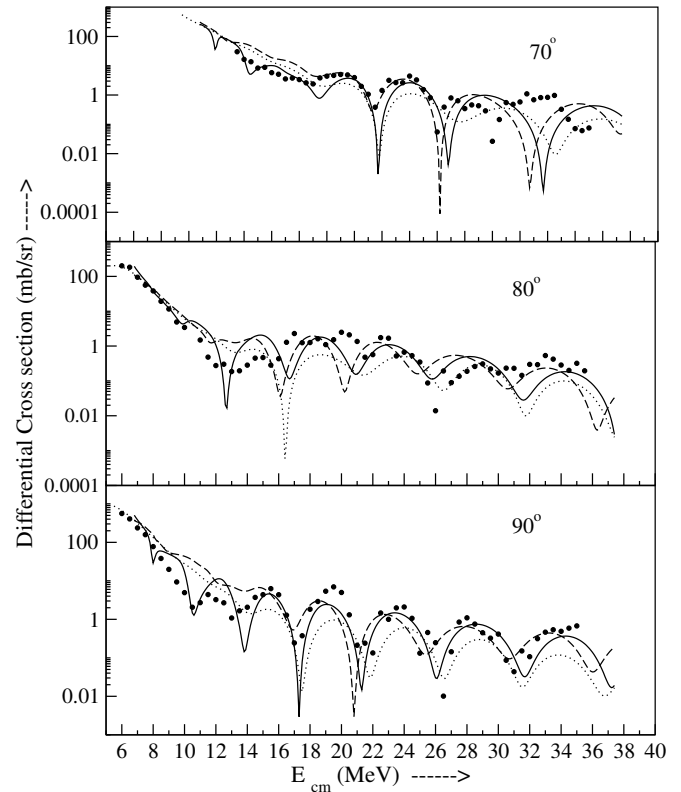


Fig. 2. Experimental and theoretical $^{14}\text{C} + ^{14}\text{C}$ elastic-scattering excitation functions at the indicated c.m. angles. The continuous, dotted and dashed curves result from the parameters as mentioned in fig. 1

function, at minima (24.75, 26.5 MeV) and at intermediate energy (25.75 MeV) are shown in fig.1. The experimental angular distributions are reproduced very well by theoretical calculations at lower energies and good description of the data has been obtained at higher energies. The calculated angular distributions corresponding to the peaks in $\theta_{\text{cm}} = 90^\circ$ excitation function agree well with the data, except at 28 MeV where the calculations underestimate the experimental cross-sections beyond about $\theta_{\text{cm}} = 75^\circ$. This seems to be an indication of the onset of refractive effects (contributions of lower l -values) in addition to the resonant effects (dominant l -values) as also mentioned by Szilner *et al.* [20] in connection with the coexistence of resonant and refractive effects in $^{14}\text{C} + ^{14}\text{C}$, $^{12}\text{C} + ^{14}\text{C}$, $^{14}\text{C} + ^{16}\text{O}$ systems. It must, however, be pointed out that the refractive effects are expected to be observed at energies above ~ 5 MeV/nucleon [20]; just above the maximum energy up to which the data are available in our case. Of course, for the $^{14}\text{C} + ^{14}\text{C}$ system more data at higher energies and over a larger angular range are required to confirm the co-existence of resonant and refractive effects. The analysis of $^{16}\text{O} + ^{14}\text{C}$ elastic scattering data at 132, 281 and 334 MeV (higher than 8 MeV/nucleon) does show that although the absorption in this system is stronger than for the case of $^{16}\text{O} + ^{12}\text{C}$ system, nevertheless the scattering maintains the refractive behavior [21].

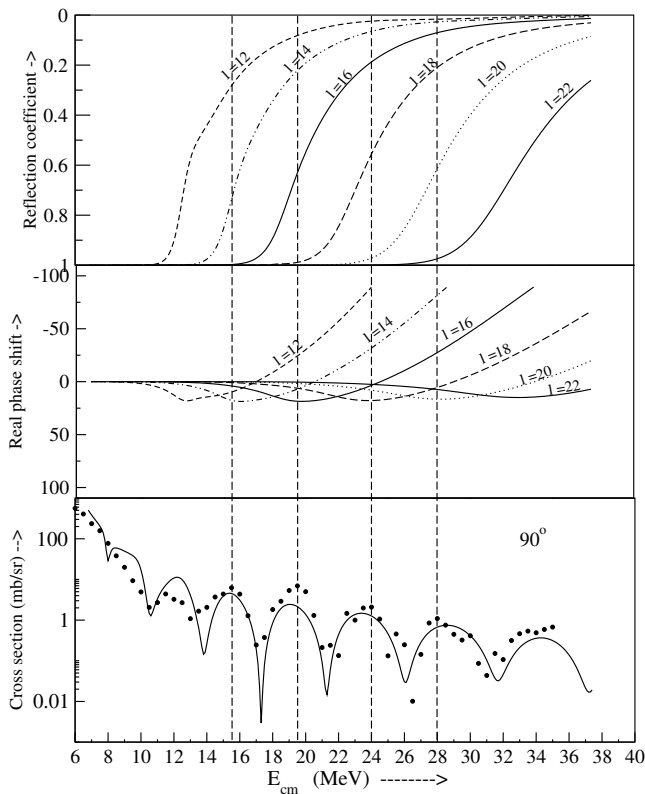


Fig. 3. The phase shifts, reflection coefficients and the 90.0° excitation functions (experimental and calculated) with distinct peaks for each partial wave.

For the purpose of comparison the corresponding optical-model calculations with the surface transparent and J -dependent shallow potentials have also been shown in fig. 1 (using Sets II and III, respectively, of table 1). These sets of parameters were obtained by fitting the data with the parameters from ref. [4] as the initial guess. It can be noted from fig. 1 that the deep potential provides better fits to the data as compared to the shallow potentials.

In fig. 2 are shown the experimental and theoretical excitation functions at the three angles. The calculations with deep potential (Set I of table 1) provide a good description of the data. In fact, the $\theta_{cm} = 90^\circ$ experimental excitation function is reproduced quite well. Thus the characteristic features of the data are well reproduced by the deep potential. The excitation functions calculated with the other two sets of potential parameters (Sets II and III of table 1) are also shown in fig. 2 for the purpose of comparison. Again it can be noted that the deep potential provides a better description of the excitation functions than the two shallow potentials and in particular at $\theta_{cm} = 90^\circ$. It might be mentioned that for the $^{16}\text{O} + ^{16}\text{O}$ system Sparenberg and Baye [22] have demonstrated that after removing complex normalizable solutions from the deep optical potential of Kondo *et al.* [9] with supersymmetric transformations, one obtains a shallow potential similar to that of Chatwin *et al.* [8]. And, therefore, it is not surprising that the deep and shallow potentials can de-

scribe the elastic data equally well for heavy-ion systems like $^{16}\text{O} + ^{16}\text{O}$ and $^{14}\text{C} + ^{14}\text{C}$.

The appearance of successive gross structure maxima in the elastic-scattering excitation functions is believed to be the consequence of an extended surface transparency of the system [7]. The physical origin of surface transparency lies in the poor angular momentum matching between the elastic channel and available reaction channels due to unfavorable Q -values [8,23]. At each energy only a few partial waves contribute, and if in addition half of these are eliminated by symmetry, like in case of the $^{14}\text{C} + ^{14}\text{C}$ system, then cross-section will be dominated by a very few partial waves one after the other as energy increases. The successive dominance of the partial waves is so marked that the excitation function may show maxima corresponding to each partial wave. The detailed phase shift analysis for $^{16}\text{O} + ^{16}\text{O}$ by Gobbi *et al.* [7] has shown that each partial wave is active only over a relatively restricted range of energy.

A similar phase shift analysis for $^{14}\text{C} + ^{14}\text{C}$ scattering (using the Set I of the potential parameters) shows a very similar behavior for the 90° excitation function. The analysis shows that, as the phase shift departs from zero, the corresponding reflection coefficient changes rapidly from unity to zero, *i.e.* from no absorption to complete absorption. Corresponding to the energy of each maxima, only one partial wave contributes significantly to elastic scattering. Further increase in energy increases the probability of absorption and hence reduces the elastic cross-section which reaches the minimum and then further increases as the next partial wave begins to contribute. The phase shift plot clearly singles out $l = 12, 14, 16, 18$ as the dominant partial waves at $E_{cm} = 15.5, 19.5, 24$ and 28 MeV, respectively (see fig. 3). As a consequence of surface transparency, the angular distributions can be fairly well reproduced by the squares of single Legendre polynomials. The above-mentioned sequence of l -values was in fact deduced for $^{14}\text{C} + ^{14}\text{C}$ scattering by comparison with the squares of single Legendre polynomials [4,5]. It may be pointed out that the phase shift plot showed more or less the same behavior even with the shallow potential (Set III) for the $^{14}\text{C} + ^{14}\text{C}$ system. And this is consistent with the point made by Sparenberg and Baye [22] that the two very different phenomenological potentials can reproduce the same data as both potentials share approximately the same cross-sections and the same phase shifts. The removal of a normalizable solution from a deep potential with a pair of supersymmetric transformations results in a shallow potential without modifying the phase shifts [22].

4 Conclusion

Although traditional shallow potentials (surface transparent and J -dependent) describe the elastic scattering angular distributions and excitation functions for $^{14}\text{C} + ^{14}\text{C}$ reasonably well (specially the J -dependent), the deep potential has been found to be more successful. In fact, the quality of fits is the same or better as obtained for systems

like $^{16}\text{O} + ^{16}\text{O}$, $^{16}\text{O} + ^{12}\text{C}$ [9,17] using the deep potentials. The present analysis further supports the validity of deep potentials for heavy-ion systems which exhibit gross structures in their elastic-scattering excitation functions.

The authors are grateful to Dr D. Konnerth for providing them with the nicely tabulated data for this analysis. They are grateful to the referee for valuable suggestions and also for drawing their attention to refs. 14, 16, 20 and 21. One of the authors (S.V.) acknowledges the financial assistance being provided by Council of Scientific and Industrial Research (CSIR), New Delhi, India.

References

1. K.A. Erb, D.A. Bromley, *Treatise on Heavy Ion Science*, edited by D.A. Bromley, Vol. **3** (Plenum, New York, 1985) p. 201.
2. R. Singh, *Nuclear Reactions*, edited by R. Singh, S.N. Mukherjee (New age International Ltd. , New Delhi, 1996) p. 206.
3. J.V. Maher, M.W. Sachs, R.H. Siemssen, A. Weidinger, D.A. Bromley, *Phys. Rev.* **188**, 1665 (1969).
4. D. Konnerth, K.G. Bernhardt, K.A. Eberhard, R. Singh, A. Strzalkowski, W. Trautmann, W. Trombik, *Phys. Rev. Lett.* **45**, 1154 (1980); D. Konnerth, W. Trombik, K.G. Bernhardt, K.A. Eberhard, R. Singh, A. Strzalkowski, W. Trautmann, *Nucl. Phys. A* **436**, 538 (1985).
5. D.M. Drake, M. Cates, N. Cindro, D. Pocanic, E. Holub, *Phys. Lett. B* **98**, 36 (1981).
6. R.M. Wieland, R.G. Stokstad, G.R. Satchler, L.D. Rickertsen, *Phys. Rev. Lett.* **37**, 1458 (1976).
7. A. Gobbi, W. Wieland, L. Chua, D. Shapira, D.A. Bromley, *Phys. Rev. C* **7**, 30 (1973).
8. R.A. Chatwin, J.S. Eck, D. Robson, A. Richter, *Phys. Rev. C* **1**, 795 (1970).
9. Y. Kondo, B.A. Robson, R. Smith, *Phys. Lett. B* **227**, 310 (1989).
10. T. Wada, H. Horiuchi, *Prog. Theor. Phys.* **80**, 488 (1988).
11. C. Gao, Y. Kondo, B.A. Robson, *Nucl. Phys. A* **529**, 234 (1991).
12. Y. Kondo, F. Michel, G. Reidemeister, *Phys. Lett. B* **242**, 340 (1990).
13. Y. Sugiyama, Y. Tomita, H. Ikezoe, Y. Yamanouchi, K. Ideno, S. Hamada, T. Sugimitzu, M. Hijiya, Y. Kondo, *Phys. Lett. B* **312**, 35 (1993).
14. M.E. Brandan, G.R. Satchler, *Phys. Rep.* **285**, 143 (1997).
15. S. Ohkubo, *Phys. At. Nuclei* **66**, 1534 (2003).
16. M.P. Nicoli, F. Haas, R.M. Freeman, N. Aissaoui, C. Beck, A. Elanique, R. Nouicer, A. Morsad, S. Szilner, Z. Basrak, M.E. Brandan, G.R. Satchler, *Phys. Rev. C* **60**, 064608 (1999).
17. C. Gao, Y. Kondo, *Phys. Lett. B* **408**, 7 (1997).
18. F.G. Perey, *Computer code GENOA-Oak Ridge National Laboratory* (unpublished, USA, 1967), modified by J.G. Cramer.
19. C. Detraz, *Annu. Rev. Nucl. Part. Sci.* **39**, 407 (1989).
20. S. Szilner, F. Haas, Z. Basrak, *Fizika B* **12**, 117 (2003).
21. A.A. Oglobin, S.A. Goncharov, Yu. A. Glukhov, A.S. Demyanova, M.V. Rozhkov, V.P. Rudakov, W.H. Trzaska, *Phys. At. Nuclei* **66**, 1523 (2003).
22. J.M. Sparenberg, D. Baye, *Phys. Rev. C* **54**, 1309 (1996).
23. F. Haas, Y. Abe, *Phys. Rev. Lett.* **46**, 1667 (1981).